Nature

INTERNATIONAL WEEKLY JOURNAL OF SCIENCE

383 No. 6602 24 October 1996 £3.00

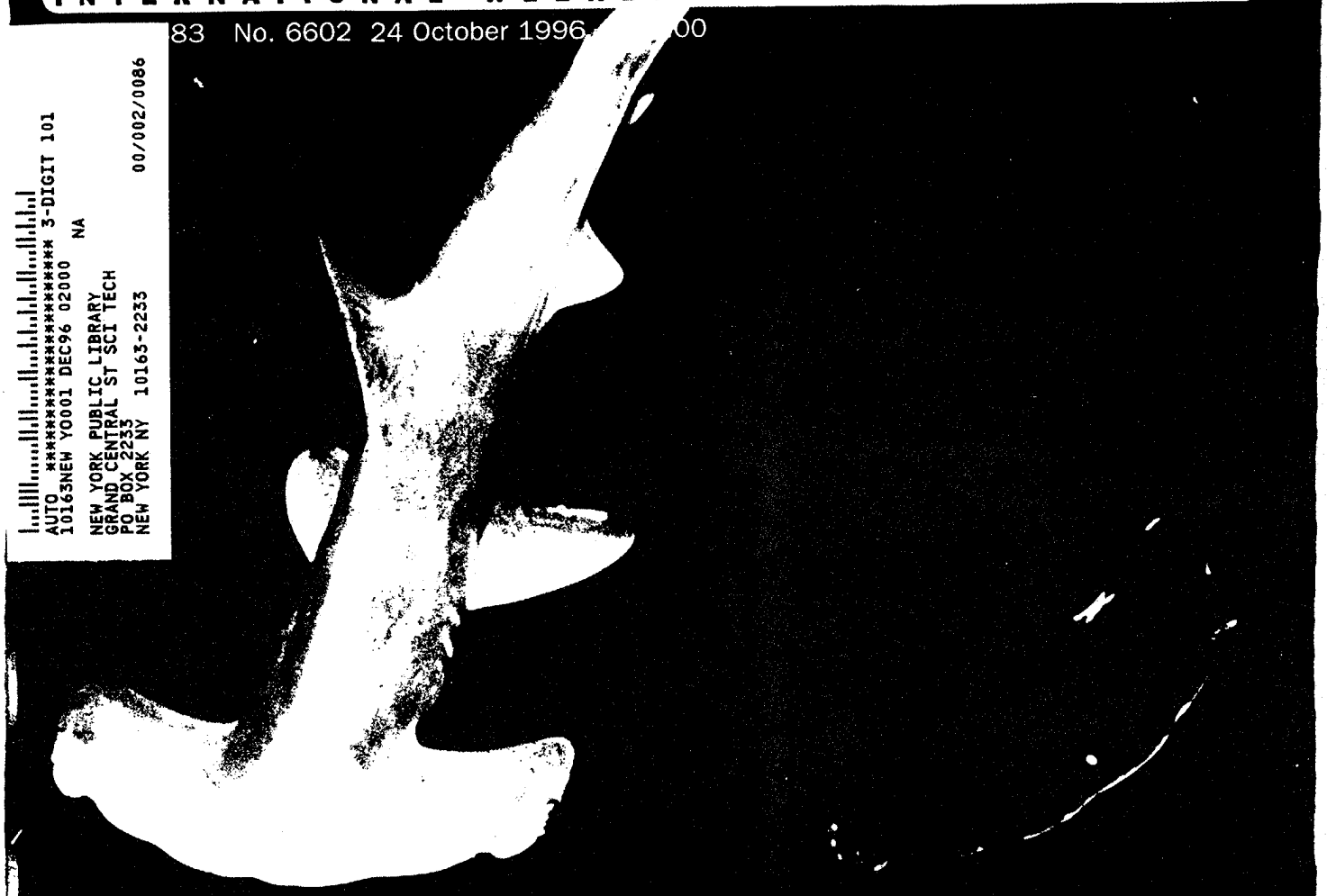

Suntanned hammerheads

receptor with different functional domains, with the intracellular domain having the intrinsic signal-transducing activity of the intact protein and the extracellular domain a regulating activity[25]. Mutations in these various domains result in different phenotypic alterations in *Drosophila*[25,26]. Interestingly, we did not notice any difference in the phenotypes of the CADASIL patients who carry mutations in EGF-like and Cdc10 domains, nor in the phenotypes of patients carrying mutations in distinct EGF domains. Further genotype/phenotype correlation studies should help to establish the function of this protein. Study of the expression of this protein and of the Notch signalling pathway in adult vascular and brain tissues will also help in understanding molecular mechanisms leading to the development of CADASIL and other cerebro-vascular diseases and dementia. The involvement of *Notch3* in CADASIL suggests that disruption of the Notch signalling pathway may be a key factor in adult-onset conditions causing dementia. □

Methods

Patients. We analysed a panel of 58 unrelated patients fulfilling clinical and neuroradiological criteria for CADASIL[2,6]. 28 of these belong to previously linked families (ref. 6, and our unpublished results); family members of the remaining patients were not available for linkage analysis. Genotyping has been described[6]. Sequences of microsatellite markers are available through the Genome Data Base (Johns Hopkins University, Baltimore).

Physical map of the CADASIL region. YAC libraries from CEPH[27] were screened by PCR with microsatellite markers *D19S885*, *D19S253*, *D19S923* and *D19S929*. YAC and BAC libraries from ICRF and Research Genetics Inc. (ref. 96055) were screened by hybridization using single-copy probes p25.1.4 (1.4-kb *Eco*RI subclone of p13.1.25; ref. 28), IMAGE cDNA clone 22368 (ref. 29), F63 (0.6-kb *Rsa*I fragment from a fetal brain cDNA clone isolated using primers of EST00679), p12HC (2-kb *Hinc*II fragment from cosmid 12909; ref. 30), F11EK (0.8-kb fragment from cosmid 11547; ref. 30). Subcloned BAC ends were isolated by hybridization of specific oligonucleotides from the left BAC end (CTC TAG AGT CGA CCT GCA GGC ATG CA) and from the right BAC end (GAT TAC GCC AAG CTA TTT AGG TGA CAC TAT AGA ATA C) to replicate filters of, respectively, Bluescript ad Puc 18 *Eco*RI libraries from each BAC. Contig assembly was established by STS and single-copy probes content. Chimaerism of YAC clones was analysed by FISH.

Identification of transcribed sequences: (1) CpG island characterization. *Not*I–*Hin*dIII libraries from BACs 13J4, 14G5 and 187L3 were constructed. Subclones were sequenced using vector primers and unique probes, prepared from these *Not*I-containing fragments, hybridized to zoo blots and northern blots. **(2) Direct cDNA selection.** Random-primed, reverse-transcribed cDNA pools from lymphoblastoid cells, fetal and adult brain were hybridized on YAC clones 766e7, 417c3 and 884g1, according to ref. 7. PCR-amplified cDNAs from a fetal brain cDNA library (Clonetech) were hybridized on YAC clone 417c3, according to ref. 8. Physical mapping of selected clones was established by hybridization to *Eco*RI-digested YAC and *Hin*dIII-digested BAC southern blots.

Characterization of the human *Notch3* gene: (1) cDNA isolation. A total of 8 cDNAs were characterized. P28-20 and CNA202 were isolated from a human fetal brain cDNA library (Clonetech, ref. HL3003a) by conventional hybridization procedures using two probes: (1) X20, a 4.1-kb mouse *Notch3* cDNA fragment, kindly provided by U. Lendahl and M. Lardelli, and (2) a 0.2-kb genomic fragment corresponding to a human *Notch3* exon N3 (see below). IMAGE cDNA clones[29] (149693, 153875, 261623) and Genexpress (c-32b03) cDNA clones were identified by computer screening the dBest database with a Blast-N algorithm, using sequences of, respectively, 884Na4, J432NH and J431NH fragments. **(2) Determination of intron–exon boundaries.** Replicates of a *Sau*3A library from BAC 13J4 were hybridized with three partial mouse *Notch3* cDNA fragments covering the whole cDNA sequence (X20, Mel3 and JJ5). Filters were hybridized in 50% formamide hybridization buffer and washed at 55 °C in 0.2× SSPE, 0.1% SDS buffer. Positive clones were sequenced using vector primers and sequences were aligned with human and mouse *Notch3* cDNA sequences. Double-strand sequencing of genomic DNA or cloned cDNA fragments was done on an ABI 377 DNA sequencer (Applied Biosystems) using dideoxy terminators. **(3) Expression analysis.** Northern blots containing human poly(A)$^+$ RNAs from various adult and fetal tissues were purchased from Clonetech (ref. 7760-1, 7756-1). Membranes were hybridized according to the manufacturer's instructions, washed at a final stringency of 0.2× SSPE, 0.1% SDS at 50 °C and exposed for 5 d at −80 °C for autoradiography.

Screening for mutations. Oligonucleotides were designed from intron–exon boundaries sequences to amplify genomic fragments of ~200 bp. Reactions were performed in a final volume of 25 µl, containing 100 ng genomic DNA, 0.5 µM of each primer, 150 µM dNTP mix, 1 × PCR *Taq* polymerase buffer (Cetus), 1 U of *Taq* polymerase (BRL), 1.5 µCi dCTP for 30 cycles of 94 °C for 15 s, 65 °C for 15 s, 72 °C for 15 s. PCR products were denatured in 50% formamide and electrophoresed through a 6% non-denaturing polyacrylamide gel. DNA from CADASIL patients showing an altered SSCP band was directly sequenced after PCR amplification.

Received 29 July; accepted 29 August 1996.

1. Tournier-Lasserve, E., Iba-Zizen, M. T., Romero, N. & Bousser, M. G. *Stroke* **22,** 1297–1302 (1991).
2. Chabriat, H. *et al. Lancet* **346,** 934–939 (1995).
3. Baudrimont, M., Dubas, F., Joutel, A., Tournier-Lasserve, E. & Bousser, M. G. *Stroke* **24,** 122–125 (1993).
4. Ruchoux, M. M. *et al. Acta Neuropathol.* **89,** 500–512 (1995).
5. Tournier-Lasserve, E. *et al. Nature Genet.* **3,** 256–259 (1993).
6. Ducros, A. *et al. Am. J. Hum. Genet.* **58,** 171–181 (1996).
7. Rommens, J. M. *et al. Hum. Mol. Genet.* **2,** 901–907 (1993).
8. Parimoo, S., Patanyali, S. R., Shukla, H., Chaplin, D. & Weissman, S. M. *Proc. Natl Acad. Sci. USA* **88,** 9623–9627 (1991).
9. Lardelli, M., Dahlstrand, J. & Lendahl, U. *Mech. Dev.* **46,** 123–136 (1994).
10. Larsson, C., Lardelli, M., White, I. & Lendahl, U. *Genomics* **24,** 253–258 (1994).
11. Wharton, K. A., Johansen, K. M., Xu, T. & Artavanis-Tsakonas, S. *Cell* **43,** 567–581 (1985).
12. Artavanis-Tsakonas, S., Matsuno, K. & Fortini, M. E. *Science* **268,** 225–232 (1995).
13. Ellisen, L. W. *et al. Cell* **66,** 649–661 (1991).
14. Stifani, S., Blaumueller, C. M., Redhead, N. J., Hill, R. E. & Artavonis-Tsakonas, S. *Nature Genet.* **2,** 119–127 (1992).
15. Kidd, S., Baylies, M. K., Gasic, G. P. & Young, M. W. *Genes Dev.* **3,** 1113–1129 (1989).
16. Rebay, I. *et al. Cell* **67,** 687–699 (1991).
17. Henderson, S. T., Gao, D., Lambie, E. J. & Kimble, J. *Development* **120,** 2913–2924 (1994).
18. Mello, C. C., Draper, B. W. & Priess, J. R. *Cell* **77,** 95–106 (1994).
19. Fortini, M. & Artavanis-Tsakonas, S. *Cell* **79,** 273–282 (1994).
20. Lindsell, C. E., Shawber, C. J., Boulter, J. & Weinmaster, G. *Cell* **80,** 909–917 (1995).
21. Mlodzik, M., Baker, N. E. & Rubin, G. M. *Genes Dev.* **4,** 1848–1861 (1990).
22. Levitan, D. & Greenwald, I. *Nature* **377,** 351–354 (1995).
23. Sherrington, R. *et al. Nature* **375,** 754–760 (1995).
24. Campbell, I. D. & Bork, P. *Curr. Opin. Struct. Biol.* **3,** 385–392 (1993).
25. Rebay, I., Fehon, R. G. & Artavanis-Tsakonas, S. *Cell* **74,** 319–329 (1993).
26. Kelley, M. R., Kidd, S., Deutsch, W. A. & Young, M. *Cell* **51,** 539–548 (1987).
27. Bellanné-Chantelot, C. *et al. Cell* **70,** 1059–1068 (1992).
28. Buroker, N. E. *et al. Hum. Genet.* **76,** 90–95 (1987).
29. Lennon, G., Auffray, C., Polymeropoulos, M. & Soares, B. *Genomics* **33,** 151–152 (1996).
30. Ashworth, L. K. *et al. Nature Genet.* **11,** 422–427 (1995).

ACKNOWLEDGEMENTS. We thank all families and clinicians for their participation; M. Lardelli and U. Lendahl for mouse *Notch3* cDNA fragments, X20, Mel3 and JJ5; H. Mohrenweiser for chromosome-19 cosmids; D. Lepaslier for CEPH YAC libraries; ICFR for ICRF YAC libraries; A. Troesch and J. Bouyer for sequencing; C. Auffray for Genexpress cDNA clones; E. Viegas-Péquignot for FISH mapping; M. Abitbol for human fetal brain; J. J. Hauw for tissues from Banque de Tissus Cryopreservés de l'hôpital de la Salpetrière; M. Baudrimont for anatomopathological analysis; J. Melki and J. M. Rommens for helpful advice. This work was supported by INSERM, bioMérieux, Association Française contre les Myopathies, Assistance Publique-Hôpitaux de Paris, Groupe de Recherche et d'Etude du Génome, Ministère de l'Enseignement Supérieur et de la Recherche, and Institute Necker.

CORRESPONDENCE and requests for materials should be addressed to E.T.-L. (e-mail: Tournier@necker.fr).

Increased amyloid-β42(43) in brains of mice expressing mutant presenilin 1

Karen Duff*†, Chris Eckman†, Cindy Zehr*†, Xin Yu*, Cristian-Mihail Prada†, Jordi Perez-tur*†, Mike Hutton*†, Luc Buee‡, Yasuo Harigaya†, Debra Yager†, David Morgan§, Marcia N. Gordon§, Leigh Holcomb§, Lawrence Refolo†, Brenda Zenk†, John Hardy*† & Steven Younkin†

* Suncoast Alzheimer's Disease Laboratories, University of South Florida, Tampa, Florida 33612, USA
† Birdsall Building, Mayo Clinic Jacksonville, 4500 San Pablo Road, Jacksonville, Florida 32224, USA
‡ Unite 422 INSERM, Place de Verdun, 50945 Lille Cedex, France
§ Alzheimer's Research Laboratory, Department of Pharmacology, University of South Florida, Tampa, Florida 33613, USA

MUTATIONS in the genes encoding amyloid-β precursor protein (*APP*)[1], presenilin 1 (*PS1*)[2] and presenilin 2 (*PS2*)[3,4] are known to cause early-onset, autosomal dominant Alzheimer's disease. Studies of plasma and fibroblasts from subjects with these mutations have established that they all alter amyloid β-protein (βAPP) processing, which normally leads to the secretion of amyloid-β protein (relative molecular mass 4,000; M_r 4K; ~90%

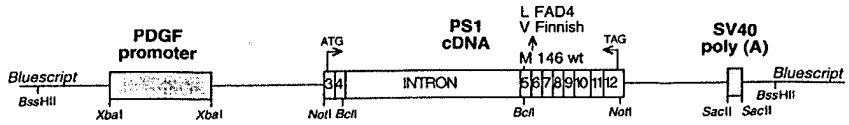

FIG. 1 Constructs for the expression of wild-type and mutant *PS1* in transgenic mice.

Aβ1–40, ~10% Aβ1–42(43)), so that the extracellular concentration of Aβ42(43) is increased[5]. This increase in Aβ42(43) is believed to be the critical change that initiates Alzheimer's disease pathogenesis because Aβ42(43) is deposited early and selectively in the senile plaques that are observed in the brains of patients with all forms of the disease. To establish that the presenilin mutations increase the amount of Aβ42(43) in the brain and to test whether presenilin mutations act as true (gain of function) dominants, we have now constructed mice expressing wild-type and mutant presenilin genes. Analysis of these mice showed that overexpression of mutant, but not wild-type, PS1 selectively increases brain Aβ42(43). These results indicate that the presenilin mutations probably cause Alzheimer's disease through a gain of deleterious function that increases the amount of Aβ42(43) in the brain.

Mice that were transgenic for wild-type or mutant *PS1* genes were generated as described (see Methods and Fig. 1). Founders were assessed by sequential Southern blotting of tail DNA, northern blotting of brain RNA and western blotting of brain proteins, to determine which lines to expand and use for experimentation. Mice expressing wild-type PS1 (4 lines), the mutation in which methionine was substituted with leucine at residue 146 (M146L)[2] (2 lines) or valine, the M146V mutation[6,7] (also 2 lines) were chosen for further analysis on the basis of their high protein levels. F_0 (3 wild-type lines) or F_1 (1 wild-type and the four mutant lines) mice were killed and their brains taken for analysis of *PS1* expression by northern blot (Fig. 2) and western blot (Fig. 3). These results showed that *PS1* messenger RNA was expressed in the transgenic mice, that the transgene was correctly spliced, and that this expression resulted in increased amounts of the ~46K PS1 holoprotein and the amino-terminal ~27K PS1 derivative, which have previously been described[8].

The brains of mice from each line were homogenized in 70% formic acid and analysed with sandwich enzyme-linked immunosorbent assays (ELISAs) specific for Aβ40 and Aβ42(43) as described previously (Table 1)[9,10]. Expression of mutant or wild-type PS1 had no significant effect on brain Aβ40, whereas expression of mutant but not wild-type PS1 increased brain Aβ42(43) (Table 1). In six non-transgenic mice, Aβ42(43) concentration was 0.36 ± 0.06 pmol per g wet tissue, and in seven mice expressing wild-type PS1 (the three founders and four F_1 mice from one of the wild-type lines), Aβ42(43) concentration was 0.50 ± 0.07 pmol per g wet tissue. In five mice expressing the PS1 M146L mutant (one founder and four F_1 mice), Aβ42(43) was increased to 0.84 ± 0.09 pmol per g wet tissue, and in nine mice expressing the PS1 M146V mutant (four F_1 mice from one line and 5 F_1 mice from the other), Aβ42(43) was increased to 0.81 ± 0.04 pmol per g wet tissue. Analysis of the six nontransgenic mice and the seven mice expressing wild-type PS1 (using the Mann-Whitney test; a conservative test that makes no assumptions about sample distribution) showed that expression of wild-type PS1 did not significantly increase the levels of Aβ42(43), even though expression of wild-type PS1 was substantially increased to levels comparable to those for mutant PS1 (Fig. 3). However, in the 14 mice expressing mutant PS1, as compared with the seven mice expressing wild-type PS1, there was a significant increase in Aβ42(43) ($P = 0.01$ for M146L, $P = 0.002$ for M146V, and $P = 0.001$ for all mutant lines combined). There was no indication in our data that the effect of the *PS1* mutations was related to expression level (Fig. 3 and Table 1). Histopathological analysis of mice at age 3–4 weeks revealed no Aβ deposition or other pathology (data not shown). Mice expressing sufficient amounts of the mutant APPs linked to familial Alzheimer's disease have been shown to deposit Aβ in senile plaques and to develop other changes like those seen in the diseased brain, but these mice do not show pathology until they are many months older[11,12]. Thus, it will be important to determine whether mice with PS1 mutations develop Aβ deposits or other abnormal phenotype as they age. It will also be of interest to determine whether breeding of these mice with mice bearing APP transgenes will lead to mice that develop Alzheimer-like pathology even if neither parental strain developed pathology on its own.

The observations reported here extend our previous findings in fibroblasts and plasma from subjects with *PS1/2* mutations in two main ways[13]. First, they show that the *PS1* mutations increase Aβ42(43) not only in peripheral cells, but also in the brain, the target organ for Alzheimer's disease pathology. Thus, they validate the use of fibroblasts as a model system to study the effect of *PS1/2* mutations on βAPP processing. Second, our results indicate that mutant presenilins might act in a truly dominant fashion because the normal endogenous *PS1* genes in mice expressing the mutant *PS1* transgene did not prevent the increase in Aβ42(43). Thus, it seems that the pathogenic *PS1* mutations act either in a dominant-negative fashion (perhaps by forming complexes that impair overall PS1 function) or through a gain of function that influences Aβ42(43). It should be noted that we could not discriminate endogenous and transgenic PS1 at the protein level in this study, although we could discriminate mutant and wild-type PS1 mRNAs (Fig. 2). Endogenous PS1 mRNA continued to be expressed even when there was marked overexpression of transgenic PS1 mRNA (Fig. 2), making it likely that there was continued expression of endogenous PS1 protein; however, we cannot rule out the possibility that endogenous PS1 was downregulated at the protein level when mutant PS1 was overexpressed. If endogenous PS1 is downregulated so that mutant PS1 replaces wild-type PS1, then the *PS1* mutations might be acting by compromising normal PS1 function. Additional measurements of endogenous PS1 in transgenic animals are needed to show conclusively that the PS1 mutation acts in a dominant fashion.

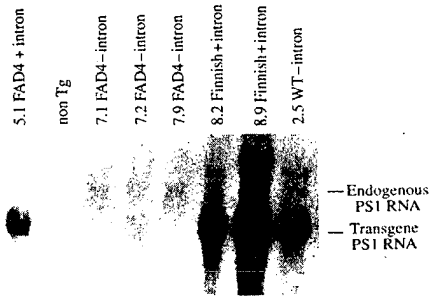

FIG. 2 Northern blot analysis of *PS1* mRNA in the brains of transgenic mice expressing wild-type or mutant *PS1*. Line numbers are given (see Table 1). The transgene mRNA band is clearly seen at ~1.6 kb as expected and the intron seems to have been spliced out correctly. A larger band at ~4 kb is also seen in transgenic animals which is thought to be a minor mRNA species arising from readthrough of the polyadenylation signal. Only the 1.6-kb transgene mRNA is translated into protein (Fig. 3). Endogenous mouse *PS1* is seen at ~3 kb. The inclusion of intron 5 generally led to greatly increased PS1 mRNA (data not shown), as has been previously reported for other transgenes[19]. With the exception of line 2.5, all lines used expressed intron-containing constructs. Tg, transgenic; WT, wild type.

TABLE 1 Analysis of Aβ in brain tissue

Transgene	Line	Animal number	Aβ40 BNT77/BA27	Aβ42(43) BNT77/BC05	Increase in Aβ42(43) (mutant–WT)
Non-transgenic		1	2.55	0.49	NA
		2	2.69	0.50	NA
		3	2.61	0.48	NA
		4	2.21	0.16	NA
		5	2.48	0.26	NA
		6	2.62	0.26	NA
		Mean ± s.e.m.	2.53 ± 0.07	0.36 ± 0.06	NA
PS1WT	4.2	1	2.76	0.46	NA
	4.7	1	4.55	0.74	NA
	2.5	1	2.31	0.54	NA
		2	2.70	0.54	NA
		3	2.90	0.58	NA
		4	2.98	0.56	NA
	4.8	1	2.35	0.11	NA
		Mean ± s.e.m.	2.94 ± 0.29	0.50 ± 0.07	NA
PS1 M146L	5.1	1	2.34	0.72	0.22
		2	2.52	0.69	0.19
		3	2.80	0.75	0.25
		4	2.97	0.89	0.39
	6.2	1	2.13	1.17	0.67
		Mean ± s.e.m.	2.55 ± 0.15	0.84 ± 0.09	0.34 ± 0.09
PS1 M146V	8.2	1	2.80	0.81	0.31
		2	3.21	0.82	0.32
		3	2.39	0.66	0.16
		4	2.56	0.76	0.26
	8.9	1	2.99	0.99	0.49
		2	2.71	0.90	0.40
		3	2.41	0.89	0.39
		4	2.62	0.81	0.31
		5	2.59	0.68	0.18
		Mean ± s.e.m.	2.70 ± 0.09	0.81 ± 0.04	0.31 ± 0.04

Aβ measurement (see text) is in pmol per g wet tissue. NA, not applicable.

Most importantly, our results indicate that presenilin-encoded Alzheimer's disease follows a pathogenic route involving Aβ42(43) that may be common to all forms of the disease. Although it is possible that there are routes other than Aβ deposition that lead to the Alzheimer's disease phenotype, the simplest explanation, that in general it follows directly from such alterations in Aβ metabolism, remains unrefuted. This offers hope for a common therapeutic strategy as it would mean that most of the pathogenic process will be common to Alzheimer's disease of different aetiologies. The connection between the presenilins and βAPP processing remains obscure, but both PS1 and PS2 are membrane-associated proteins, generally predicted to have seven transmembrane domains, found in the Golgi[14], and which are similar to two *C. elegans* proteins, *Sel*-12 (ref. 15) and *Spe*-4 (ref. 8), that are involved in cell fate determination through the *lin-12/Notch* signalling pathway and spermatogenesis, respectively. The involvement of *Spe*-4 in protein trafficking in the Golgi during spermatogenesis[16] means that any interactions between the presenilins and βAPP in this compartment might be a fruitful area of study[17]. □

Methods

Transgene construction. The PDGFβ2 promoter was amplified by polymerase chain reaction (PCR) from the clone psisCAT6a (ref. 18) between the *Xba*I and the *Avr*II site converting the latter to an *Xba*I site. This promoter directs neuronal expression in the CNS[11,18]. The 1.4-kb human *PS1* coding sequence (from the ATG start to the TAG stop site, lacking bases that encode the alternately spliced VRSQ motif[6]) was amplified by PCR using primers that incorporated *Not*I sites at both ends and a modified 5′ Kozak sequence. A 224-bp fragment of the SV40 containing the polyadenylation signal site was amplified to incorporate *Sac*II sites using pβNASS (Clontech) as a template. The three fragments were cloned into their corresponding sites in pBluescriptII SK⁻ (Stratagene). A 2.8-kb intron between exons 4 and 5 was PCR-amplified from a human *PS1* PAC clone 54-12D (ref. 5) (Genome Systems). The intron was digested with *Bcl*I and cloned into the transgene at the *Bcl*I sites located in exons 4 and 5. The Transformer mutagenesis system (Clontech) was used to convert the wild-type sequence to M146L and M146V. Plasmid DNA was prepared using Qiagen Qiatip 100 columns and sequenced throughout. Constructs were removed from the vector by digestion with *Bss*HII, gel purification and clean up using a Wizard PCR column (Promega). DNA was eluted from the column into TE (10 mM Tris buffer, pH. 7.4, 0.1 mM EDTA) and diluted to 3–5 ng μl^{-1} in this buffer.

Generation and maintenance of transgenic mice. DNA was injected into fertilized eggs from a Swiss Webster (SW) (Taconic) × B6D2 F_1 cross. Mice expressing 5 different constructs were generated: *PS1* WT (M146) with and without intron 5, M145L with and without intron 5 and M146V with intron 5. Subsequent generations were produced by breeding founders with B6D2 or SW.

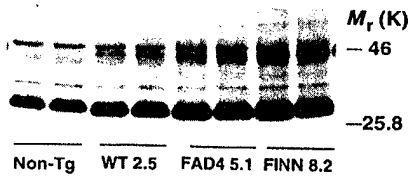

FIG. 3 Western blot analysis of PS1 in the brains of transgenic mice expressing wild-type or mutant PS1. In non-transgenic mice only the ~27K N-terminal PS1 derivative was detected. In transgenic mice expressing either wild-type or mutant PS1, there was marked overexpression of both the ~46K holoprotein and ~27K PS1 N-terminal derivative. Labelling of both the ~46K and ~27K proteins was specific because it was abolished by absorption with the cognate peptide, but labelling of the ~52K protein was not abolished, indicating that this protein is non-specifically labelled. All transgenic lines analysed for Aβ (Table 1) were compared on western blots (like those shown above) with equal amounts of brain lysates applied to adjacent wells. The relative amounts of ~46K holoprotein and ~27K N-terminal derivative were: WT line 4.7 < WT line 4.2 = WT line 2.5 slightly < M146L line 5.1 = WT line 4.8 = M146V line 8.2 < M146L line 6.2 = M146V line 8.9.

No difference in Aβ levels was observed in F_1 generations derived by crossing (SW × SW/B6D2 F_1) or (SW/B6D2 F_1 × B6D2 F_1).

Analysis of transgenic mice. To identify founders, DNA was extracted from the tails of 10 day old mice using a Genomic DNA isolation kit (Promega). DNA (10 μg) was digested overnight with *Eco*RI, Southern blotted and hybridized in Quick-Hyb (Stratagene) at 68 °C for 1 hour with a ^{32}P-labelled *PS1* complementary probe. Blots were exposed to film overnight. For northern blot analysis of mouse brains, RNA was extracted from one cerebral hemisphere of two-week-old pups using trizol reagent (Gibco/BRL). RNA was transferred to Hybond N (Amersham) as described for Southern blotting.

PCR primers and conditions. The primers used were: PDGF F, 60 °C annealing, 5′ GAT CTC TAG AGG ATC CAC AG; PDGF/*Xba*R, 5′ GAC TCT AGA GAG GCA GC; SV40 F, 5′ CAT GTC GAC TAG GCG GCC GCG GGG ATC; SV40/*Sac*II R, 5′ CAT CCG CGG TCG ACT CTA GAG A; Intron 5 F, 51 °C annealing, 5′ AAG ATG AGG AAG AAG ATG; Intron 5 R, 5′ CCC AAC CAT AAG AAG AAC AG; *PS1*/*Not*I/Kozak F, 65 °C annealing, 5′ GGC GAG CGG CCG CAC CTG CTC CGG CCA TGA CAG AGT TAC CTG CAC CA; *PS1*/*Not*I R, 5′ CCG CTG CGG CCG CGG ATT CTA ACC GCA AAT ATG C. All PCRs were run under standard conditions (High Fidelity Taq polymerase, Boehringer, 94 °C for 5 minutes X1, then (94 °C for 30 s, annealing temperature, for 30 s, 72 °C for 30–45 s) X30, followed by 72 °C X1 for 5 min) except for the *PS1*/*Not*I/Kozak F amplification, where the cycling extension time was increased to 5 m.

Western blot analysis. A peptide corresponding to the PS1 sequence (T2–N12) was synthesized. Two additional basic amino acids (arginine and lysine) were added to the carboxy terminus of the peptide, to increase its solubility. An additional cysteine residue was also added to conjugate the peptide to a protein carrier (ovalbumin) using m-maleimidobenzoyl-*N*-hydroxysuccinimide ester (MBS). The conjugated peptide (180 μg) TC14. (TELPA-PLSYF-NRKC-NH_2) together with Freund's complete adjuvant, was emulsified and injected intradermally into 15–20 sites along the sides of New Zealand rabbits. Every three weeks, the rabbits were immunized using Freund's incomplete adjuvant. Ten days after the further immunization the rabbits were bled.

Mouse brain was Dounce-homogenized at a ratio of 150 mg tissue per ml of homogenization buffer (2% SDS in saline solution) containing a complete protease inhibitor cocktail (Boehringer Mannheim) and sonicated 4 times for 10 s at 50 W and 70% amplitude, using a microsonic cell disrupter (Kontes). The homogenate was spun at 35,000 *g* for 30 min and the supernatant was transferred to a separate tube for analysis. Protein concentration was determined using the BCA protein determination kit (Pierce). Before loading, the samples were diluted 1:1 in 2× tricine sample buffer (Novex) containing 1% dithiothreitol. Samples were not heated before loading. The gels were elctrophoresed for ~1.5 h at 125 V and transferred to Immobilon (Millipore). After blocking with 5% milk in TBS the blots were incubated with a 1:1,000 dilution of anti-PS1 antibody and detected with HRP-linked anti-rabbit secondary antibody using ECL (Amersham).

Analysis of Aβ in brain tissue. Tissue (150 mg) was Dounce-homogenized (6 strokes) in 1 ml of 70% formic acid. Homogenates were centrifuged at 100,000 *g* for 1 h. The supernatant was recovered and neutralized by a 20-fold dilution in 1 M Tris base. A sample (100 ml) was mixed with 50 ml of buffer EC (0.02 M sodium phosphate, 0.2 mM EDTA, 0.4 M NaCl, 0.2% BSA, 0.05% CHAPS, 0.4% Block-Ace, 0.05% sodium azide, pH 7.0) and analysed directly using the BNT77/BA27 or BNT77/BC05 sandwich ELISA systems[20,21]. The capture antibody (BNT77) used here was raised against amino acids 11–28 of the Aβ peptide sequence. The values reported were calculated by comparison with a standard curve of synthetic human Aβ1-40 and Aβ1-42 (Bachem).

Histology. Anaesthetized mice were perfused with paraformaldehyde and horizontal brain sections were immunocytochemically stained for Aβ using the 4G8 antibody (Senetek, St Louis, MO) both with and without formic acid pretreatment.

Received 27 August; accepted 25 September 1996.

1. Goate, A. *et al. Nature* **349,** 704–706 (1991).
2. Sherrington, R. *et al. Nature* **375,** 754–760 (1995).
3. Levy-Lahad, E. *et al. Science* **269,** 973–977 (1995).
4. Rogaev, E. *et al. Nature* **376,** 775–778 (1995).
5. Suzuki, N. *et al. Science* **264,** 1335–1340 (1994).
6. Alzheimer's Disease Collaborative Group *Nature Genet.* **11,** 219–222 (1995).
7. Haltia, M. *et al. Ann. Neurol.* **36,** 362–367 (1994).
8. Thinakaran, G. *et al. Neuron* **17,** 181–190 (1996).
9. Iwatsubo, T. *et al. Ann. Neurol.* **37,** 294–299 (1995).
10. Gravina, S. A. *et al. J. Biol. Chem.* **270,** 7013–7016 (1995).
11. Games, D. *Nature* **373,** 523–527 (1995).
12. Hsiao, K. *et al. Science* (in the press).
13. Scheuner, D. *et al. Nature Med.* **2,** 864–870 (1996).
14. Kovacs, D. M. *et al. Nature Med.* **2,** 224–229 (1996).
15. Levitan, D. & Greewald, I. *Nature* **377,** 351–354 (1996).
16. L'Hernault, S. W. & Arduengo, P. M. *J. Cell Biol.* **119,** 55–68 (1992).
17. Xu, H., Greengard, P. & Gandy, S. *J. Biol. Chem.* **270,** 23243–23245 (1995).
18. Sasahara, M. *et al. Cell* **64,** 217–227 (1991).
19. Brinster, R. *et al. Proc. Natl Acad. Sci. USA* **85,** 836–840 (1988).
20. Suzuki, N. *et al. Am. J. Path.* **145,** 452–460 (1994).
21. Odaka, N. *et al. Biochemistry* **34,** 10272–10278 (1995).

ACKNOWLEDGEMENTS. This work was supported by an NIA Program Project grant to K.D., M.H., D.G., S.Y. and J.H. and Alzheimer's Association and American Health Assistance Foundation grants. We thank T. Collins for the gift of the PDGF promoter; N. Suzuki and A. Odeka of Takeda Industries for the BNT77, BA-27 and BC-05 antibodies; N. Irving for modifying the *PS1* cDNA; S. Prusiner, D. Foster, M. Guitierrez and W. Balkan for allowing K.D. to use their facilities for training; R. Engelman and S. Manetta for animal husbandry; and E. Eckman and L. Younkin for comments on the manuscript.

CORRESPONDENCE should be addressed to J.H. (e-mail: hardy.john@mayo.edu). Requests for materials to K.D. at the Mayor Clinic (e-mail: duff.karen@mayo.edu).

Hippocampal synaptic transmission enhanced by low concentrations of nicotine

Richard Gray†, Arun S. Rajan*, Kristofer A. Radcliffe†, Masuhide Yakehiro† & John A. Dani†

* Department of Medicine and † Division of Neuroscience, Baylor College of Medicine, Houston, Texas 77030-3498, USA

NICOTINE obtained from tobacco can improve learning and memory on various tasks and has been linked to arousal, attention, rapid information processing, working memory, and long-term memories that can cause craving years after someone has stopped smoking[1,2]. One likely target for these effects is the hippocampus, a centre for learning and memory that has rich cholinergic innervation and dense nicotinic acetylcholine receptor (nAChR) expression[3–6]. During Alzheimer's dementia there are fewer nAChRs and the cholinergic inputs to the hippocampus degenerate[7]. However, there is no evidence for fast synaptic transmission mediated by nAChRs in the hippocampus, and their role is not understood[8,9]. Nicotine is known to act on presynaptic nAChRs within the habenula of chick to enhance glutamatergic transmission[10]; here we report that a similar mechanism operates in the hippocampus. Measurements of intracellular Ca^{2+} in single mossy-fibre presynaptic terminals indicate that nAChRs containing the α7 subunit can mediate a Ca^{2+} influx that is sufficient to induce vesicular neurotransmitter release. We propose that nicotine from tobacco influences cognition by enhancing synaptic transmission. Conversely, a decreased efficacy of transmission may account for the deficits associated with the loss of cholinergic innervation during Alzheimer's disease.

After a cigarette has been smoked, nicotine in arterial blood can reach a concentration of about 0.5 μM, and the drug is delivered to the brain less than 10 s after absorption in the lungs[11]. To investigate the role of hippocampal nAChRs, we applied 0.5 μM nicotine to hippocampal cultures or pressure-puffed a low concentration onto hippocampal slices. CA3 pyramidal neurons in the rat hippocampal slice respond to nicotine with an increased rate of spontaneous miniature excitatory postsynaptic currents (mEPSCs) (Fig. 1*a*). Voltage-dependent Ca^{2+} channels were blocked by 200 μM Cd^{2+}, and action potentials were inhibited by 1 μM tetrodotoxin (TTX). In those experiments, a pyramidal neuron from the CA3 region was patch-clamped in the whole-cell mode, and a pipette was positioned to apply a local pressure puff of bath solution containing 20 μM nicotine onto the dendrites of the CA3 neuron. The actual concentration of nicotine that reached the nAChRs was much less than 20 μM. The frequency but not the amplitude of mEPSCs increased in all four of the CA3 neurons that were tested (Fig. 1*b*). The time course of the frequency increase depended on the position of the puffer pipette, the depth of the neuron in the slice, and the removal of nicotine by diffusion and by wash out of the bath (1 ml min^{-1} in a 0.6-ml chamber).

To control precisely the concentration of applied nicotine, we examined rat hippocampal neurons in tissue culture plated at a low density or on micro-islands. Nicotine (0.5 μM) was applied to